DOI: 10.1002/ejic.200601156

Anomeric Interactions in Pentafluoroethylimidosulfurous Dichloride, $CF_3CF_2N{=}SCl_2$: Structural, Conformational and Configurational Properties in the Gaseous and Condensed Phases

Norma L. Robles,[a][‡] Rosa M. S. Álvarez,[a][‡‡] Edgardo H. Cutin,[a][‡‡] Carlos O. Della Védova,*[b,c][‡‡] Mauricio F. Erben,[b][‡‡] Roland Boese,[d] Helge Willner,[e] and Rüdiger Mews[f]

Keywords: Imides / Conformation analysis / Structural analysis / Hyperconjugation / Sulfur

The structural, conformational, and configurational properties of pentafluoroethylimidosulfurous dichloride ($CF_3CF_2N{=}SCl_2$) have been studied by vibrational spectroscopy [IR (vapor) and Raman (liquid)] and quantum chemical calculations [HF, B3LYP and MP2 approximations using the 6-311+G(d) and 6-311+G(2df) basis sets]. $CF_3CF_2N{=}SCl_2$ exists in the liquid phase as a single (*Z*) form (C–N bond synperiplanar with respect to the Cl–S–Cl plane; C_1 symmetry). The structure was also determined by X-ray diffraction analysis of a single crystal grown in situ at low temperature. The crystalline solid at 159 K (monoclinic, $P2_1/c$, a = 5.2466(10), b = 15.376(3), c = 18.730(3) Å, β = 96.391(3)°, Z = 8) consists of two crystallographically inequivalent (*Z*) forms. The results are discussed in terms of both hyperconjugative electronic effects and of natural bond orbital (NBO) calculations.

Introduction

Theoretical studies performed in the last twenty years have concluded that more than one single effect should be considered in order to understand the factors stabilizing the staggered conformation of ethane. Hyperconjugation, or the anomeric effect, which is a stereoelectronic effect derived from the overlap of σ-bonding orbitals with an adjacent empty or partially filled antibonding orbital, has been proposed as the most significant factor responsible for stabilizing staggered ethane in a definite molecular conformation.[1–3] This concept has also been applied to fluoroethane species,[4] which have recently attracted much attention, and ultrafast carbon–carbon single-bond isomerization of 1-fluoro-2-isocyanatoethane in solution at room-temperature has been analyzed by two-dimensional infrared vibrational echo spectroscopy.[5]

It is well known that conjugation between lone-pair orbitals and π bonds plays an important role in structural chemistry (the resonance effect) and that the conformational preference is strongly influenced by the presence of perfluorinated groups.[6,7] For instance, conjugation in methyl vinyl ether [$CH_3OC(H){=}CH_2$][8–10] results in a sterically unfavorable synperiplanar orientation of the O–C(sp^3) bond relative to the double bond, whereas the O–C(sp^3) bond in $CF_3OC(F){=}CF_2$[11] is nearly perpendicular to the plane of the vinyl group [ϕ(C=C–O–C) = 104(2)°]. An orbital interaction occurs between the oxygen lone-pair orbital and the π*(C=C) antibonding orbital [lpπ(O)→π*(C=C)] in $CH_3OC(H){=}CH_2$, whereas no conjugation is present in the perfluorinated compound.

Structural, configurational, and conformational studies in compounds such as sulfur imides ($R^1NSR^2R^3$)[12] are scarce, and little is known about the factors affecting these properties. In principle, depending on the orientation of the R^1–N bond with respect to the R^2–S–R^3 bisector angle, two forms [(*E*)/(*Z*)] can be expected (Scheme 1).

[a] Instituto de Química Física, Facultad de Bioquímica, Química y Farmacia, Universidad Nacional de Tucumán, San Lorenzo 456, 4000 Tucumán, Argentina
[b] CEQUINOR (CONICET-UNLP). Departamento de Química, Facultad de Ciencias Exactas, Universidad Nacional de La Plata, 47 esq. 115 (B1900AJL) C. C. 962, La Plata, Buenos Aires, Argentina
E-mail: carlosdv@quimica.unlp.edu.ar
[c] Laboratorio de Servicios a la Industria y al Sistema Científico (UNLP-CIC-CONICET), Camino Centenario, Gonnet, Buenos Aires, Argentina
[d] Institut für Anorganische Chemie, Universität Duisburg-Essen, Universitätsstrasse 5–7, 45117 Essen, Germany
[e] FB C, Anorganische Chemie, Bergische Universität Wuppertal, Gaußstrasse 20, 42119 Wuppertal, Germany
[f] Institut für Anorganische und Physikalische Chemie, Universität Bremen, 28334 Bremen, Germany
[‡] N. L. R. is a doctoral fellow of CONICET.
[‡‡]R. M. S. Á., E. H. C., M. F. E. and C. O. D. V. are members of the Carrera del Investigador of CONICET, República Argentina.

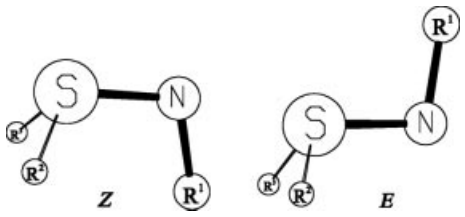

Scheme 1. Representation of the (*Z*) and (*E*) forms of $R^1NSR^2R^3$.

Vibrational spectroscopy, gas electron diffraction, X-ray crystallography, quantum chemical calculations, and other techniques have proved to be powerful tools to understand the structural properties of sulfur imide molecules containing fluorine atoms or fluorinated substituents groups. Thus, the structure and conformational and configurational properties of molecules of the type $R_FN{=}SF_2$ [R_F = CF_3,[13–16] FC(O),[17,18] NC,[19] $CF_3C(O)$,[20] and FSO_2[21,22]] and $R_FN{=}SCl_2$ [R_F = CF_3[23,24] and FC(O)[25]] have been studied, all of which show only a (*Z*) configuration around the putative N=S double bond. It is interesting to note that compounds with different substituents attached at the sulfur atom of the N=S group favor the (*E*) form. Thus, FC(O)N=S(F)CF_3[26] and $CF_3C(O)N{=}S(F)CF_3$[27] exist in the vapor as a mixture of (*E*) and (*Z*) forms, with the former predominating.

The question of the nature of the S–N bond in sulfur imides has not yet been resolved, and there is still some controversy as to whether the sulfur imide linkage is a double bond or a semipolar bond.[28] As noted by Protashchuk et al.[29] the relative stabilization of the (*Z*) and (*E*) forms of the simple molecule $HNSH_2$ depends mainly on the effectiveness of the following interactions: (1) the lone pair attached at the nitrogen atom with the σ* antibonding orbitals of the SH_2 fragment [lp(N)→σ*(S–H)], (2) the lone pair of the sulfur atom with the σ* antibonding orbital of the NH fragment [lp(S)→σ*(N–H)], and (3) the lone pairs of the nitrogen and sulfur atoms with each other. Both the stabilizing [(1) and (2)] and destabilizing [(3)] interactions are more effective in the (*Z*) than in the (*E*) form, and the destabilizing interaction energy between both lone pairs attached at the nitrogen and sulfur atoms in the (*Z*) form is lower than the stabilizing effects of the negative hyperconjugation, which results in the greater stability of the (*Z*) form for $HNSH_2$. A quantitative evaluation of these effects has been reported recently by Kumar et al.[30] for $HNSH_2$ and also for fluorinated derivatives, by using the NBO population analysis approach.

In order to gain additional experimental and theoretical information about the structural properties of sulfur imides, we report here a study of $CF_3CF_2N{=}SCl_2$ species that draws on its vibrational spectra [IR (vapor) and Raman (liquid)] and single-crystal structure. The presence of the CF_3CF_2 group is useful to analyze the effect of a fully fluorinated carbon chain on the molecular structure. Moreover, quantum chemical calculations have been performed in order to assist the interpretation of the experimental data, and Natural Bond Orbital (NBO) population analyses have been applied to rationalize the effect of electronic interactions on the structural, conformational, and configurational properties of $CF_3CF_2N{=}SCl_2$.

Results and Discussion

Quantum Chemical Calculations

According to the precedents found in the literature for *S*,*S*-dihalo-substituted sulfur imides $R_1N{=}SX_2$ (X = F, Cl; see above), the presence of the (*Z*) form might be expected for $CF_3CF_2N{=}SCl_2$. In order to gain further insight into this molecule, the potential function for internal rotation around the sulfur–imide bond was calculated by geometry optimizations at fixed torsional dihedral angles (steps of 30°) using the HF, B3LYP, and MP2 methods with the 6-311+G(d) basis sets. The derived curves obtained with the HF and MP2 approximations show two minima: a global minimum that corresponds to the (*Z*) structure and a local minimum located about 7.5 kcal mol^{-1} higher in energy which corresponds to the (*E*) form of $CF_3CF_2N{=}SCl_2$ [(*Z*) and (*E*) orientation of the C–N bond with respect to the Cl–S–Cl bisector angle, respectively]. A more complicated picture of the potential energy surface for the mentioned angles was obtained by the hybrid method B3LYP, which shows the same global minimum structure as the former approximations but with a flat region near the local minimum assigned to the (*E*) form. Similar calculations performed by varying the dihedral angle around the C–N bond showed only one minimum at about –150°. Thus, both (*Z*) and (*E*) forms belong to the C_1 symmetry point group. Full geometry optimizations and frequency calculations for the two feasible conformers were performed with the more extended 6-311+G(2df) basis sets. The relative energies are summarized in Table 1.

Table 1. Calculated relative energies (corrected for the zero-point energy) in kcal mol^{-1} for stable conformers of $CF_3CF_2N{=}SCl_2$.

	HF/6-311+G(d) $\Delta E°$[a]	B3LYP/6-311+G(d) $\Delta E°$[a]	MP2/6-311+G(d) $\Delta E°$[a,b]
syn	0.00	0.00	0.00
anti	5.55	7.34	7.62

[a] Energy differences $\Delta E° = E°_{(E)} - E°_{(Z)}$. [b] Zero-point corrections calculated at the B3LYP/6-311+G(d) level.

Since the perfluoroethyl group (CF_3CF_2) can adopt either a staggered or an eclipsed geometry (see Scheme 2),

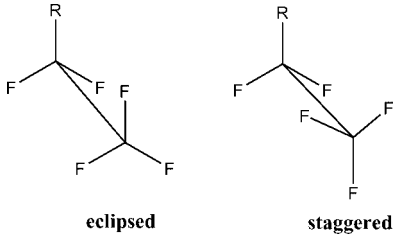

Scheme 2. Representation of the eclipsed and staggered forms in substituted perfluoroethane molecules.

the potential function for internal rotation around the C–C bond was calculated by full geometry optimization at fixed ϕ(FC–CN) torsional angles. The staggered form corresponds to the preferred conformation, with ΔE ($E_{eclipsed} - E_{staggered}$) values of 5.67 and 4.10 kcal mol^{-1} for the HF and B3LYP methods with the 6-311+G* basis set, respectively.

Vibrational Spectra

Figure 1 shows the IR (vapor) and Raman (liquid) spectra of $CF_3CF_2N{=}SCl_2$. Table 2 lists the experimental frequencies together with the calculated values and a tentative assignment of the 27 expected normal modes of vibration. The vibrational spectra can be interpreted satisfactorily on the basis of the presence of only one form. Assignment of the bands related to the $N{=}SCl_2$ moiety was performed on the basis of the corresponding features for similar *S*,*S*-dichlorosulfur imide derivatives such as $CF_3N{=}SCl_2$,[23] $FC(O)N{=}SCl_2$,[25] and $ClSO_2N{=}SCl_2$.[31] The corresponding *S*,*S*-difluoro derivatives $CF_3N{=}SF_2$,[32] $FC(O)N{=}SF_2$,[23] and $ClSO_2N{=}SF_2$[22] were also taken into account to establish a correlation between the different modes. The fundamental vibrational modes related to the CF_3CF_2 moiety were assigned on the basis of calculated frequencies for the title molecule and taking into account the recently reported data for CF_3CF_2COOH.[33] All theoretical frequencies show good agreement with the experimental values, which gives confidence to the assignment of the fundamental features.

According to reported data found in the literature for sulfur imide molecules containing a CF_3 group as substituent, the region between 1400 and 1100 cm^{-1} shows bands related to the fundamental stretching modes corresponding to both the N=S and the CF_3 groups.[23,32] Thus, the presence of several intense and narrow bands in that region in the gas FTIR spectra and weak and broad bands in the liquid Raman spectrum is directly related to those vibrational modes. The frequency of the N=S stretching is directly related to the electron-withdrawing properties of the substituents attached at the nitrogen and sulfur atoms. In fact, an increase in the electron-withdrawing properties of the substituents attached to any of the atoms of the N=S bond increases the bond order of this bond. Taking into account that the band centered at 1314 cm^{-1} in the IR spectrum (1300 cm^{-1}, Raman) of $CF_3N{=}SCl_2$[23] was assigned to the N=S stretching, and postulating that the CF_3 group is more electronegative than CF_3CF_2, the band appearing at 1292 cm^{-1} in the gas FTIR spectrum (1286 cm^{-1} in the liquid Raman spectrum) was assigned to the N=S stretching vibration, in perfect agreement with the theoretical

Table 2. Observed and calculated vibrational data for $CF_3CF_2N{=}SCl_2$ [cm^{-1}].

Mode	Approximate description[a]	Experimental[b]				Calculated[c]			
		IR (gas)		Raman (liquid)		HF/ 6-311+G(2df)[d]		B3LYP/ 6-311+G(2df)	
ν_1	C–C stretch	1380	(20)	1378	(5)	1403	(2)	1365	(16)
ν_2	N=S stretch	1292	(98)	1286	(6)	1292	(100)	1292	(100)
ν_3	CF_3 sym stretch	1235	(100)	1218	(2)	1262	(31)	1212	(31)
ν_4	CF_3 asym stretch					1256	(22)	1210	(40)
ν_5	CF_2 asym stretch	1158	(65)	1151	(2)	1183	(24)	1122	(24)
ν_6	CF_3 sym stretch	1133	(76)	1124	(2)	1143	(31)	1116	(27)
ν_7	CF_2 sym stretch	1029	(78)	1025	(3)	1027	(18)	1028	(29)
ν_8	C–N stretch	770	(2)	771	(36)	767	(<1)	766	(<1)
ν_9	CF_3 sym def	709	(47)	709	(3)	709	(12)	708	(15)
ν_{10}	C_2F_5 asym def	622	(3)	626	(3)	620	(<1)	613	(<1)
ν_{11}	C_2F_5 sym def	582	(10)	584	(3)	581	(2)	576	(2)
ν_{12}	C_2F_5 asym def	544	(6)	545	(3)	544	(2)	539	(3)
ν_{13}	C_2F_5 sym def	501	(6)	–	–	517	(3)	521	(1)
ν_{14}	SCl_2 sym stretch	442	(4)	445	(100)	460	(10)	434	(10)
ν_{15}	SCl_2 asym stretch	429	(60)	424 sh	(42)	456	(15)	413	(14)
ν_{16}	C_2F_5 sym def			395	(48)	400	(2)	391	(4)
ν_{17}	C_2F_5 sym def			362 sh	(9)	391	(2)	384	(8)
ν_{18}	C_2F_5 asym def			–		357	(<1)	354	(1)
ν_{19}	SCl_2 wag			298	(42)	295	(<1)	291	(2)
ν_{20}	SCl_2 twis			242 sh	(24)	247	(<1)	227	(<1)
ν_{21}	C_2F_5 asym def			–		220	(<1)	215	(<1)
ν_{22}	SCl_2 sym def			206	(62)	209	(<1)	196	(<1)
ν_{23}	C–C–N def			156	(44)	149	(<1)	142	(<1)
ν_{24}	C–N–S def			115	(42)	112	<1)	95	(<1)
ν_{25}	SCl_2 torsion			82	(32)	72	(<1)	75	(<1)
ν_{26}	CF_3 torsion					55	(<1)	53	(<1)
ν_{27}	C–N torsion					15	(<1)	11	(<1)

[a] Stretch = stretching, def = deformation, wag = wagging, twis = twisting, sym = symmetric, asym = asymmetric, sh = shoulder; see Figure 2 for atom numbering. [b] Gas: P = 15.0 mbar (glass cell, 200 mm optical path length, Si windows, 0.5 mm thick), relative absorbance at band maximum in parentheses; liquid: room temperature, relative band intensity in parentheses. [c] Relative band strength in parentheses; 100%: 968 and 703 km mol^{-1} for the (*Z*) form calculated at the HF and B3LYP methods, respectively. [d] Scaled by a factor of 0.9.

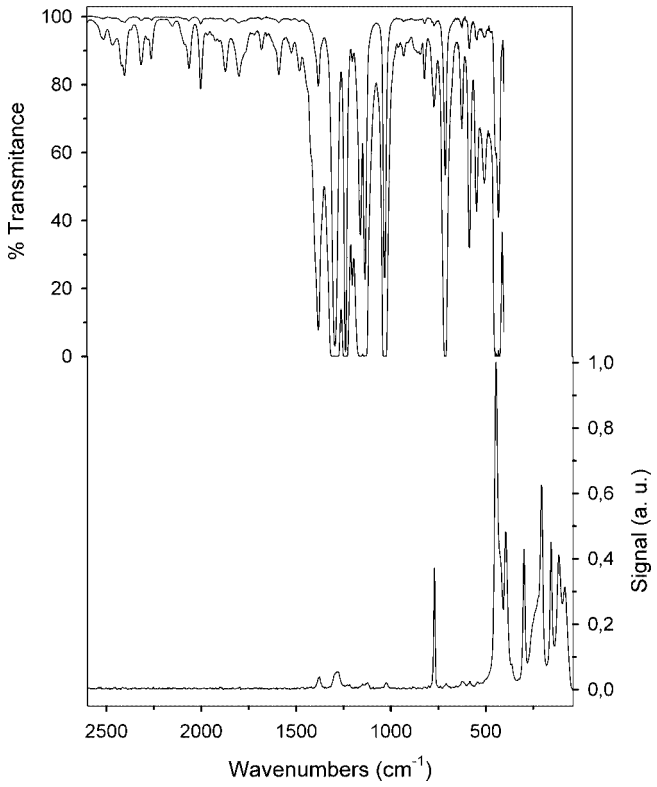

Figure 1. Gas IR (at 15.0 and 1.6 mbar; glass cell with a 200 mm optical path length and 0.5 mm thick Si windows) and liquid Raman spectra for $CF_3CF_2N{=}SCl_2$.

value. Analysis of the IR spectra obtained for seven alkyl esters of pentafluoropropionic acid [$CF_3CF_2C(O)OR$] by Crowder[34] concluded that different R groups do not affect the characteristic stretching and deformation frequency values of the CF_3CF_2 group. Thus, taking into account the reported data for CF_3CF_2COOH,[33] where the band located at 1334.7 cm^{-1} in the gas FTIR spectrum has been assigned to the C–C stretching mode, the medium intensity feature centered at 1380 cm^{-1} in the IR spectrum (Raman: 1378 cm^{-1}) of $CF_3CF_2N{=}SCl_2$ can be assigned to the ν(C–C) stretching mode.

Although theoretical calculations predict a strong coupling between the stretching modes belonging to the CF_3CF_2 group, their assignments were performed by considering the CF_3 and CF_2 groups individually. Only one band is found for the CF_3 symmetric and the antisymmetric stretching vibrational normal modes at 1235 and 1218 cm^{-1} in the vapor IR and liquid Raman spectra, respectively. This coincidence in the frequencies of these two modes is also in agreement with our calculations as differences of 6 and 2 cm^{-1} are calculated (HF and B3LYP methods, respectively) for the values of the two normal vibrational modes (Table 2). The second CF_3 symmetric stretching appears at 1133 and 1124 cm^{-1} (vapor IR and liquid Raman, respectively). Similarly, the bands centered at 1158 and 1029 cm^{-1} (Raman: 1151 and 1025 cm^{-1}) were assigned to the antisymmetric and symmetric stretching modes belonging to the CF_2 group, respectively. The medium-intensity bands observed in the IR spectrum at 442 and 429 cm^{-1} (Raman: 445 and 424 cm^{-1}) were assigned to the symmetric and antisymmetric stretching modes in the SCl_2 group, respectively. This assignment is straightforward because the frequency values as well as the shape of the bands in the vibrational spectra of $CF_3CF_2N{=}SCl_2$ can be directly correlated with the reported features for $CF_3N{=}SCl_2$.[23] Theoretical values also confirm this proposed assignment. The medium-intensity bands found at 770 and 771 cm^{-1} in the IR and Raman spectra, respectively, were assigned to the C–N stretching mode. The theoretical values calculated for this mode (HF: 767 cm^{-1}; B3LYP: 766 cm^{-1}) again support this assignment.

According to our calculated frequencies, the expected deformation modes related to the CF_3CF_2 group are strongly coupled. For this reason, it is not possible to assign the observed features in the vibrational spectra in a straightforward manner. However, by comparison with the assignment reported for $CF_3N{=}SCl_2$,[23] the band located at 709 cm^{-1} in both the IR and Raman spectra could be assigned to the totally symmetric deformation of the CF_3 group.

Crystal Structure

$CF_3CF_2N{=}SCl_2$ crystallizes in the monoclinic space group $P2_1/c$ with eight molecules per unit cell. Table 3 lists the relevant crystal data. In accordance with the theoretical calculations and the spectroscopic investigations, the most stable conformer – the (*Z*) conformer – is observed in the solid state at 159 K (Figure 2). Two nonequivalent molecules are present in the crystal (forms I and II), both of which have similar bond lengths and angles. However, some remarkable differences in the ϕ(C–C–N=S) torsional angles between both nonequivalent forms are observed. Thus, these values are 146.5° and 160.6° for forms I and II, respectively. In order to illustrate this difference, Figure 3 shows a superimposed picture of both forms.

Table 4 lists the experimental geometrical parameters for $CF_3CF_2N{=}SCl_2$ together with the corresponding values obtained from HF and B3LYP calculations using the 6-311+G(2df) basis set, and the MP2/6-311+G(d) approximation. Contractions of polar bonds are expected on going from the gas to the solid phase. Nevertheless, taking into account the difference in the physical state of the substance, there is good agreement between the theoretical and the experimental data obtained for the (*Z*) conformer of $CF_3CF_2N{=}SCl_2$. The methods reproduce the bond lengths and angles reasonably well in general, except for some values around the sulfur atom. Thus, even with large basis sets (6-311+G(2df)), the B3LYP and MP2 methods predict the S–Cl bond to be too long by up to 0.060 and 0.074 Å, respectively. The theoretical methods used in the current work give similar values for the CN=SCl dihedral angle to those obtained from the X-ray analysis. A staggered conformation for the perfluoroethyl group is found in the crystal, which is well reproduced by the computational methods. However, some differences were observed for the CC–N=S

Table 3. Crystal data and structure refinement for $CF_3CF_2N{=}SCl_2$.

Empirical formula	$C_2Cl_2F_5NS$
Formula mass	235.99
Density (calcd.) [g cm^{-3}]	2.088
F(000)	912
Temperature [K]	159(2)
Crystal size [mm]	0.3
Crystal color	colorless
Crystal description	cylindrical
Wavelength [Å]	0.71073
Crystal system	monoclinic
Space group	$P2_1/c$
a [Å]	5.2466(10)
b [Å]	15.376(3)
c [Å]	18.730(3)
α [°]	90
β [°]	96.391(3)
γ [°]	90
Volume [Å^3]	1501.6(5)
Z	8
Cell measurement reflections used	3134
Cell measurement $\theta_{min/max}$ [°]	2.19–28.22
Completeness to θ = 28.27° [%]	68.5
Index ranges	$-3 \le h \le 3$
	$-20 \le k \le 13$
	$-24 \le l \le 24$
Absorption coefficient [mm^{-1}]	1.166
Max./min. transmission	1.00/0.84
R(merg) before/after correction	0.0316/0.0195
Reflections collected	5893
Independent reflections [$R_{(int)}$ = 0.0206]	2540
Data/restraints/parameters	2150/0/199
Goodness-of-fit on F^2	1.047
Final R indices [$I > 2\sigma(I)$]	R_1 = 0.0319, wR_2 = 0.0794[a]
R indices (all data)	R_1 = 0.0393, wR_2 = 0.0837[a]
Largest diff. peak/hole [e Å^{-3}]	0.703/–0.536

[a] $w = 1/[\sigma^2(F_o^2) + (0.0313P)^2 + 1.2107P]$, where $P = (F_o^2 + 2F_c^2)/3$.

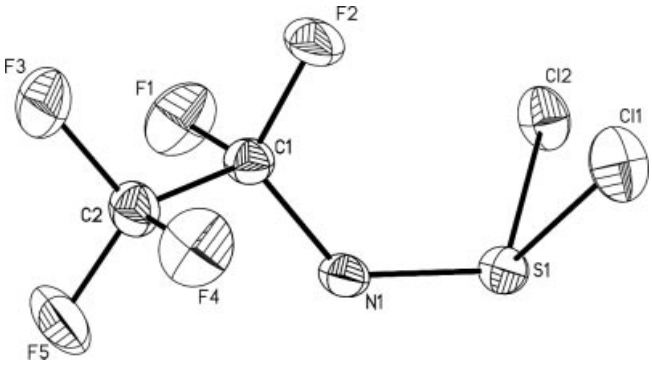

Figure 2. Molecular model, with atom numbering, showing the single-crystal structure of $CF_3CF_2N{=}SCl_2$.

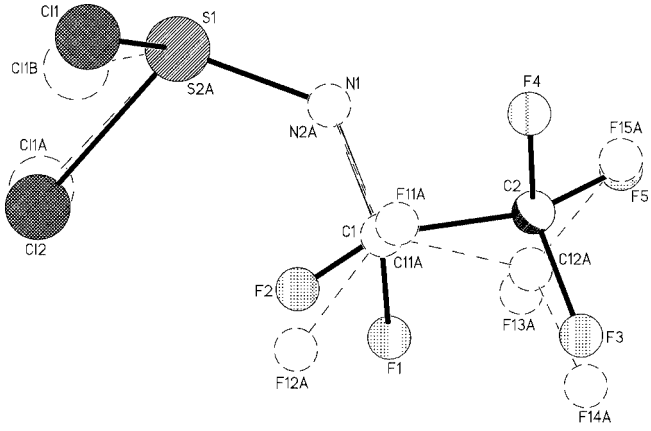

Figure 3. Molecular structures for nonequivalent forms of $CF_3CF_2N{=}SCl_2$ in the crystal.

dihedral angle: the experimental value is –147.0° whereas the computed values are –151.3°, –168.5°, and –123.7° for the HF, B3LYP, and MP2 methods, respectively.

The crystal packing along the *ac* plane is shown in Figure 4. Crystallographic studies on molecules containing halogen–halogen bonds or halogen–halogen contacts have attracted a great deal of attention because they are considered to be one of the important factors that determine the structural features in molecular crystals and may play an important role in crystal engineering as supermolecular synthons.[35–37] The term "halogen bonding" has been defined by Legon to refer to these interactions.[38] Intermolecular interactions dominated by F···F contacts are also common for fluorinated molecules where there is no other choice for stabilizing the packing. According to quantum chemical calculations, F···F contacts in aromatic systems

Table 4. Experimental and calculated geometric parameters for the Z form of $CF_3CF_2N{=}SCl_2$.[a]

Parameter	X-ray[b]	HF 6-311+G(2df)	B3LYP 6-311+G(2df)	MP2 6-311+G(d)
C1–F	1.342(3)	1.324	1.354	1.331
C–C	1.530(4)	1.538	1.558	1.543
C2–F	1.316(4)	1.304	1.333	1.348
C–N	1.399(4)	1.400	1.410	1.422
N=S	1.507(2)	1.488	1.510	1.513
S–Cl	2.072(10)	2.054	2.132	2.146
C–C–N	110.5(2)	110.0	109.6	109.4
C–N=S	129.13(18)	130.7	132.9	130.1
N=S–Cl	110.98(10)	111.0	111.7	111.4
Cl–S–Cl	95.78(4)	96.7	96.5	96.2
C–C–N=S	–147.0(3)	–151.3	–168.5	–123.7
C–N=S–Cl1	56.1(5)	60.0	49.7	53.6
C–N=S–Cl2	–49.3(5)	–46.3	–57.1	–52.5

[a] Bond lengths in Å and angles in °. See Figure 2 for atom numbering. [b] Mean values for parameters that are not unique, with σ uncertainties.

can contribute up to 14 kcal mol^{-1} of local stabilization energy.[39] The two independent molecules in the crystal of $CF_3CF_2N{=}SCl_2$ are linked to the surrounding molecules by different intermolecular interactions. For example, $CF_3CF_2N{=}SCl_2$ forms chains with short N=S···F–CF nonbonding distances along the *a* axis. These chains formed by molecules in form I show an S1···F1′ distance of 3.168 Å, whereas their analogues in form II (S2···F12′) are slightly longer (3.222 Å). The chains form a parallel array in the *ab* plane. These planes are interconnected with each other in the *c* axis orientation through two distances, an S···N′ electrostatic interaction at 3.315 Å and a Cl···Cl′ nonbonding distance of 3.479 Å (Figure 5).

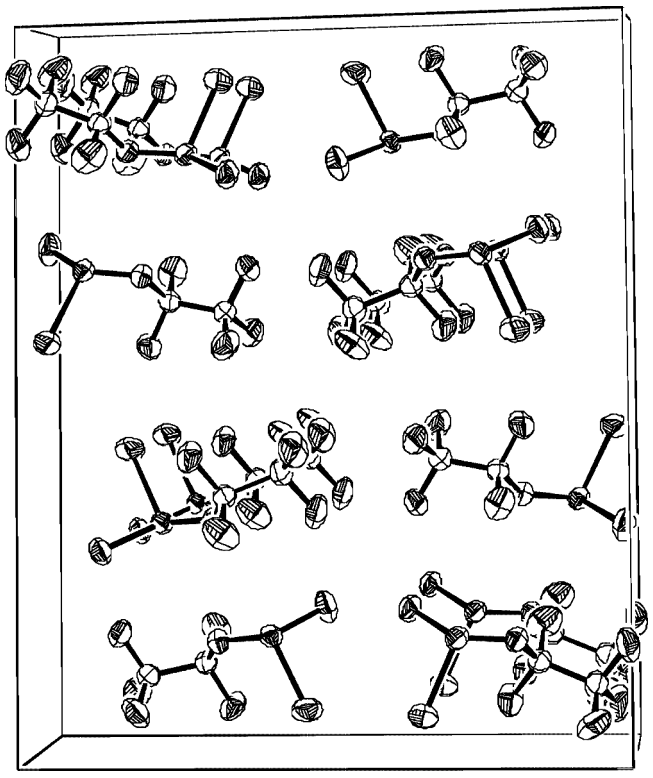

Figure 4. Stereoscopic illustration of the crystal packing of $CF_3CF_2N{=}SCl_2$ at 159 K.

Natural Bond Orbital Analysis

NBO analysis for the (*Z*) form of the $CF_3CF_2N{=}SCl_2$ molecule suggests that the formal N=S double bond has only σ-bond character. Indeed, this analysis clearly indicates the presence of two lone-pair orbitals at the nitrogen atom. The nature of these two orbitals is sp^2- [lp(Nsp^2)] and pure p-type [lp(Np)]. Their electron occupancies are low: 1.83 and 1.67 e, respectively, thus indicating the electron-donating capacity of both orbitals, in agreement with the experimental evidence relating the sulfur imide bond order with the electron-withdrawing properties of the substituents attached at the nitrogen and sulfur atoms. Delocalizing interactions evaluated by a second-order perturbation approach reveal that the first lone-pair orbital contributes to a negative hyperconjugative interaction with the S–Cl σ-antibonding orbitals [lp(Nsp^2)→σ*(S–Cl)], with a stabilizing energy $E^{(2)}$ of 37.71 kcal mol^{-1}. The second lone-pair orbital contributes to two stronger lp(Np)→σ*(S–Cl) negative hyperconjugative interactions ($E^{(2)}$ = 97.46 kcal mol^{-1}). This interaction corresponds to an electron donation from the formally doubly occupied HOMO to the vacant LUMO in $CF_3CF_2N{=}SCl_2$. Thus, the energy difference between lp(Np)→σ*(S–Cl) and lp(Nsp^2)→σ*(S–Cl) interactions is mainly related to the different denominator in the expression

$$\Delta E^{(2)}_{\phi\phi^*} = -2\frac{\left\langle \phi \middle| \hat{F} \middle| \phi^* \right\rangle^2}{\varepsilon_{\phi^*} - \varepsilon_{\phi}}$$

in which $\hat{F}$ is the Fock operator, ϕ and ϕ^* the donating and acceptor orbitals, respectively, and ε the NBO orbital energy.

This strong electron donation into the σ*(S–Cl) antibonding orbitals is also reflected in the high electronic occupancy of the σ*(S–Cl) orbital of about 0.23 e. The lone-pair orbital at the sulfur atom, on the other hand, donates electron density mainly into the vacant C–N antibonding orbital by a negative hyperconjugation interaction, lp(S)→σ*(C–N), with an $E^{(2)}$ value of 10.82 kcal mol^{-1}. All these anomeric interactions decrease on going from the (*Z*)

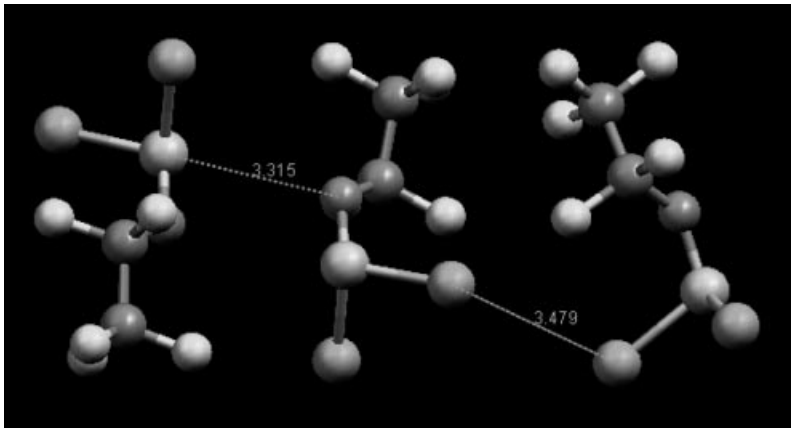

Figure 5. Short nonbonding distances in crystalline $CF_3CF_2N{=}SCl_2$ at 159 K.

to the (*E*) form, similar to the behavior calculated for H_2SNH.[30] Thus, the thermodynamic preference of the (*Z*) form for $CF_3CF_2N{=}SCl_2$ can be rationalized as originating from the dominant influence of the stabilizing anomeric interactions.

The atomic charges obtained using the Natural Population Analysis (NPA) approach for (*Z*)-$CF_3CF_2NSCl_2$ reveal that a strong positive charge (+1.25) is located at the sulfur and almost a unit negative charge (–0.99) at the nitrogen atom. These data indicate that, in addition to the negative hyperconjugation, the semipolar character of the S–N bond in sulfur imides can be attributed to this polar attraction rather than to an S–N dπ-pπ orbital interaction. It is known that the S–N rotational barrier in sulfur imide species is expected to be small in comparison with the formal double bonds depicted in their formulae because of the hypervalent nature of the sulfur atom.[40] This value has been estimated to be 8.50 kcal mol^{-1} (after including thermal corrections at the G2 level) for the simple molecule $HNSH_2$.[30] This value increases for the *S*,*S*-disubstituted sulfur imides $HN{-}SX_2$ (X = F, Cl, and Me) mainly due to the fact that the S–N bond strength increases with an enhancement in the electronegativity of the substituent bonded to the sulfur atom. Following this trend, the torsional transition state calculated for $CF_3CF_2NSCl_2$ amounts to 8.45 kcal mol^{-1} [B3LYP/6-311+G(d)], a value which is compatible with the rotational barrier expected for sulfur imides.[41]

Conclusions

Only the (*Z*) conformer around the sulfur imide bond is observed in both gaseous and condensed $CF_3CF_2N{=}SCl_2$. This structural behavior seems to be a general feature in *S*,*S*-difluoro- and *S*,*S*-dichloro-substituted sulfur imides, whereas for related compounds with two different substituents attached at the sulfur atom the (*E*) conformer is favored. The conformational and configurational properties of these molecules can be rationalized on the basis of the anomeric effect, mainly by invoking electron-donating interactions between the sulfur and nitrogen lone-pair orbitals to opposite σ* orbitals. Thus, the sterically unfavorable (*Z*) orientation is stereoelectronically stabilized mainly by lp(N)→σ*(S–Cl) and, to a minor extent, by lp(S)→σ*(N–C) interactions.

The description of the central sulfur imide bond from the NBO analysis agrees with a semipolar $S^+{-}N^-$ bond with strong hyperconjugative interactions. This analysis indicates a negatively charged nitrogen atom with two lone pairs for the $CF_3CF_2NSCl_2$ molecule, in which the sulfur atom is sp^3-hybridized. Thus, valence expansion to more than eight electrons at the sulfur atom can be excluded to explain the bonding. An inspection of the orbital shapes involved in the sulfur imide bond is given in Figure 6, which supports a redistribution of the electronic density from the negatively charged nitrogen atom to the S–N bond. These findings are in agreement with MO calculations on second-row atoms in "hypervalent" molecules. Theoretical studies of SO_2, a molecule with the sulfur atom possessing the same formal oxidation state of +IV as in $CF_3CF_2N{=}SCl_2$, show that the S–O bond has a highly ionic character, the octet rule is not violated, and it is not necessary to invoke the term "hypervalency".[42]

Experimental Section

Synthesis: $CF_3CF_2N{=}SCl_2$ was prepared by the reaction between $AlCl_3$ and $CF_3CF_2N{=}SF_2$ according to a literature procedure.[43] The product was purified by several trap-to-trap distillations.

Vibrational Spectroscopy: Gas-phase IR spectra were recorded with a resolution of 1 cm^{-1} in the range 4000–400 cm^{-1} with a Bruker IFS 66v FTIR instrument. FT Raman spectra of liquid $CF_3CF_2N{=}SCl_2$ were recorded with a Bruker RFS 100/S FT Raman spectrometer. The sample in a 6-mm (o.d.) glass tube was excited with 150 mW from a 1064-nm Nd:YAG laser (ADLAS, DPY 301, Lübeck, Germany).

X-ray Diffraction at Low Temperature: An appropriate crystal of $CF_3CF_2N{=}SCl_2$ about 0.3 mm in diameter was obtained on the diffractometer at a temperature of 159(2) K with a miniature zone-melting procedure using focused infrared laser radiation.[44] The diffraction intensities were measured at low temperature with a Nicolet R3m/V four-circle diffractometer. Intensities were collected with graphite-monochromatized Mo-K_α radiation using the ω-scan technique. The crystallographic data, conditions, and some features of the structure are listed in Table 3. The structure was solved by Patterson syntheses, and refined by the full-matrix least-squares method on *F* with the SHELTXL-Plus program.[45] All atoms were assigned to anisotropic thermal parameters. Atomic coordinates, equivalent isotropic displacement coefficients, and anisotropic displacement parameters ($Å^2 \times 10^3$) for $CF_3CF_2N{=}SCl_2$ have been deposited; further details of the crystal structure investigation may be obtained from the Fachinformationzentrum Karlsruhe, 76344 Eggenstien-Leopoldshafen, Germany (Fax: +49-7247-808-666; E-mail: crysdata@fiz-karlsruhe.de) on quoting the depository number CSD-417110.

Theoretical Calculations: All the quantum chemical calculations were performed using the GAUSSIAN03 program.[46] Geometry optimizations were performed with the HF and MP2 approximations and the B3LYP methods using 6-311+G(d) and 6-311+G(2df) basis sets and standard gradient techniques with simultaneous relaxation of all the geometric parameters. Natural population analysis and second-order donor→acceptor interaction energies were estimated at the MP2/6-31+G(d) level by using the NBO analysis[47] as implemented in the GAUSSIAN03 program.

Figure 6. NBO orbitals [MP2/6-31+G(d)] for the sulfur imide bond of $CF_3CF_2N{=}SCl_2$: (a) lp(Np), MO = 57 (HOMO); (b) lp(Nsp^2), MO = 54; (c) lp(S) MO = 39; (d) σ(N–S) MO = 34.

Acknowledgments

Financial support by the Volkswagen Stiftung (I/78724) is gratefully acknowledged. The Argentinean authors acknowledge the Fundación Antorchas, the Alexander von Humboldt Stiftung, the Deutscher Akademischer Austauschdienst (DAAD), Germany, the Agencia Nacional de Promoción Científica y Técnica (ANPCYT), the Consejo Nacional de Investigaciones Científicas y Técnicas (CONICET), the Comisión de Investigaciones de la Provincia de Buenos Aires (CIC), the Facultad de Ciencias Exactas (UNLP), and the Universidad Nacional de Tucumán (UNT). C. O. D. V. specially acknowledges the DAAD, which generously sponsors the DAAD Regional Program of Chemistry of the Republic of Argentina and supports Latin-American students earning their PhDs in La Plata.

[1] F. Weinhold, *Nature* **2001**, *411*, 539–541.
[2] V. Pophristic, L. Goodman, *Nature* **2001**, *411*, 565–568.
[3] P. R. Schreiner, *Angew. Chem. Int. Ed.* **2002**, *41*, 3579–3581.
[4] L. Goodman, H. Gu, V. Pophristic, *J. Phys. Chem. A* **2005**, *109*, 1223–1229.
[5] J. Zheng, K. Kwak, J. Xie, M. D. Fayer, *Science* **2006**, *313*, 1951–1955.
[6] F. Trautner, T. Abe, H. Oberhammer, *J. Am. Chem. Soc.* **2001**, *123*, 2865–2869.
[7] A. Hermann, F. Trautner, K. Gholivand, S. von Ahsen, E. L. Varetti, C. O. Della Védova, H. Willner, H. Oberhammer, *Inorg. Chem.* **2001**, *40*, 3979–3985.
[8] N. L. Owen, H. M. Seip, *Chem. Phys. Lett.* **1970**, *5*, 162–164.
[9] S. Samdal, H. M. Seip, *J. Mol. Struct.* **1975**, *28*, 193–203.
[10] M. Fujitake, M. Hayashi, *J. Mol. Struct.* **1985**, *127*, 21–33.
[11] C. Leibold, S. Reinemann, R. Minkwitz, P. R. Resnik, H. Oberhammer, *J. Org. Chem.* **1997**, *62*, 6160–6163.
[12] International Union of Pure and Applied Chemistry, *Nomenclature of Organic Chemistry IUPAC*, Butterworths, London, **1965**, section C.
[13] J. E. Griffiths, D. F. Sturman, *Spectrochim. Acta Part A* **1969**, *25*, 1355–1363.
[14] F. Trautner, D. Christen, R. Mews, H. Oberhammer, *J. Mol. Struct.* **2000**, *525*, 135–139.
[15] N. L. Robles, E. H. Cutín, C. O. Della Védova, *J. Mol. Struct.* **2006**, *784*, 265–268.
[16] R. R. Karl, J. S. H. Bauer, *Inorg. Chem.* **1975**, *14*, 1859–1861.
[17] C. Leibold, E. Cutin, C. O. Della Védova, H.-G. Mack, R. Mews, H. Oberhammer, *J. Mol. Struct.* **1996**, *375*, 207–211.
[18] R. M. S. Álvarez, E. H. Cutin, R. M. Romano, C. O. Della Védova, *Spectrochim. Acta Part A* **1996**, *52*, 667–673.
[19] R. S. M. Alvarez, E. H. Cutin, C. O. Della Vedova, R. Mews, R. Haist, H. Oberhammer, *Inorg. Chem.* **2001**, *40*, 5188–5191.
[20] M. I. Mora Valdez, E. H. Cutin, C. O. Della Védova, R. Mews, H. Oberhammer, *J. Mol. Struct.* **2002**, *607*, 207–215.
[21] R. Haist, R. S. M. Alvaréz, E. H. Cutin, C. O. Della Védova, H. Oberhammer, *J. Mol. Struct.* **1999**, *484*, 249–257.
[22] R. M. S. Álvarez, E. H. Cutín, R. M. Romano, H.-G. Mack, C. O. Della Védova, *J. Mol. Struct.* **1998**, *443*, 155–161.
[23] R. M. S. Alvarez, E. H. Cutin, R. M. Romano, C. O. Della Védova, *Spectrochim. Acta Part A* **1999**, *55*, 2615–2622.
[24] R. Haist, E. H. Cutin, C. O. Della Védova, H. Oberhammer, *J. Mol. Struct.* **1999**, *475*, 273–277.
[25] C. Leibold, R. M. S. Álvarez, E. H. Cutin, C. O. Della Védova, H. Oberhammer, *Inorg. Chem.* **2003**, *42*, 4071–4075.
[26] F. Trautner, E. H. Cutin, C. O. Della Védova, R. Mews, H. Oberhammer, *Inorg. Chem.* **2000**, *39*, 4833–4837.
[27] A. Hermann, M. I. Mora-Valdez, E. H. Cutin, C. O. Della Védova, H. Oberhammer, *J. Phys. Chem. A* **2003**, *107*, 7874–7878.
[28] D. Leusser, J. Henn, N. Kocher, B. Engels, D. Stalke, *J. Am. Chem. Soc.* **2004**, *126*, 1781–1793.
[29] S. I. Protashchuk, N. P. Bezverkhii, A. V. Prosyanik, *J. Struct. Chem.* **1991**, *32*, 963–965.
[30] P. S. Kumar, P. Singh, P. Uppal, P. V. Bharatam, *Bull. Chem. Soc. Jpn.* **2005**, *78*, 1417–1424.
[31] R. M. S. Álvarez, E. H. Cutin, R. M. Romano, H. G. Mack, C. O. Della Védova, *J. Raman Spectrosc.* **1998**, *29*, 257–261.
[32] N. L. Robles, E. H. Cutin, C. O. Della Védova, *J. Mol. Struct.* **2006**, *784*, 265–268.
[33] N. Rontu, V. Vaida, *J. Mol. Spectrosc.* **2006**, *237*, 19–26.
[34] G. A. Crowder, *J. Fluorine Chem.* **1973**, *2*, 217–224.
[35] J. A. R. P. Sarma, G. R. Desiraju, *Acc. Chem. Res.* **1986**, *19*, 222–228.
[36] M. B. Zaman, K. A. Udachin, J. A. Ripmeester, *Cryst. Growth Des.* **2004**, *4*, 585–589.
[37] A. Matsumoto, T. Tanaka, T. Tsubouchi, K. Tashiro, S. Saragai, S. Nakamoto, *J. Am. Chem. Soc.* **2002**, *124*, 8891–8902.
[38] A. C. Legon, *Angew. Chem. Int. Ed.* **1999**, *38*, 2686–2714.
[39] C. F. Matta, N. Castillo, R. J. Boyd, *J. Phys. Chem. A* **2005**, *109*, 3669–3681.
[40] A. E. Reed, P. v. R. Schleyer, *J. Am. Chem. Soc.* **1990**, *112*, 1434–1445.
[41] T. L. Gilchrist, C. J. Moody, *Chem. Rev.* **1977**, *77*, 409–435.
[42] J. Cioslowski, S. T. Mixon, *Inorg. Chem.* **1993**, *32*, 3209–3216.
[43] M. Lustig, *Inorg. Chem.* **1966**, *5*, 1317–1319.
[44] R. Boese, M. Nussbaumer, "In situ crystallization Techniques", in *Organic Crystal Chemistry* (Ed.: D. W. Jones), Oxford University Press, Oxford, UK, **1994**, pp. 20–37.
[45] *SHELTX-Plus Version SGI IRIS Indigo, a Complex Software Package for Solving, Refining and Displaying Crystal Structures*, Siemens, Germany, **1991**.
[46] M. J. Frisch, G. W. Trucks, H. B. Schlegel, G. E. Scuseria, M. A. Robb, J. R. Cheeseman, J. A. Montgomery Jr, T. Vreven, K. N. Kudin, J. C. Burant, J. M. Millam, S. S. Iyengar, J. Tomasi, V. Barone, B. Mennucci, M. Cossi, G. Scalmani, N. Rega, G. A. Petersson, H. Nakatsuji, M. Hada, M. Ehara, K. Toyota, R. Fukuda, J. Hasegawa, M. Ishida, T. Nakajima, Y. Honda, O. Kitao, H. Nakai, M. Klene, X. Li, J. E. Knox, H. P. Hratchian, J. B. Cross, C. Adamo, J. Jaramillo, R. Gomperts, R. E. Stratmann, O. Yazyev, A. J. Austin, R. Cammi, C. Pomelli, J. W. Ochterski, P. Y. Ayala, K. Morokuma, G. A. Voth, P. Salvador, J. J. Dannenberg, V. G. Zakrzewski, S. Dapprich, A. D. Daniels, M. C. Strain, O. Farkas, D. K. Malick, A. D. Rabuck, K. Raghavachari, J. B. Foresman, J. V. Ortiz, Q. Cui, A. G. Baboul, S. Clifford, J. Cioslowski, B. B. Stefanov, G. Liu, A. Liashenko, P. Piskorz, I. Komaromi, R. L. Martin, D. J. Fox, T. Keith, M. A. Al-Laham, C. Y. Peng, A. Nanayakkara, M. Challacombe, P. M. W. Gill, B. Johnson, W. Chen, M. W. Wong, C. Gonzalez, J. A. Pople, *GAUSSIAN03*, Revision B.04 ed., Gaussian, Inc., Pittsburgh, PA, **2003**.
[47] A. E. Reed, L. A. Curtiss, F. Weinhold, *Chem. Rev.* **1988**, *88*, 899–926.

Received: December 7, 2006
Published Online: June 19, 2007

